Driven low density granular mixtures

Riccardo Pagnani,[1,2] Umberto Marini Bettolo Marconi,[3,4] Andrea Puglisi[1,2]
[1]*Dipartimento di Fisica, Università "La Sapienza," Piazzale Aldo Moro 2, 00198 Roma, Italy*
[2]*Istituto Nazionale di Fisica della Materia, Unità di Roma, Roma, Italy*
[3]*Dipartimento di Fisica, Università di Camerino, 62032 Camerino, Italy*
[4]*Istituto Nazionale di Fisica della Materia, Unità di Camerino, Camerino, Italy*
(Received 29 May 2002; revised manuscript received 19 July 2002; published 19 November 2002)

We study the steady state properties of a two-dimensional granular mixture in the presence of energy driving by employing simple analytical estimates and direct simulation Monte Carlo. We adopt two different driving mechanisms, (a) a homogeneous heat bath with friction and (b) a vibrating boundary (thermal or harmonic) in the presence of gravity. The main findings are the appearance of two different granular temperatures, one for each species; the existence of overpopulated tails in the velocity distribution functions and of nontrivial spatial correlations indicating the spontaneous formation of cluster aggregates. In the case of a fluid subject to gravity and to a vibrating boundary, both densities and temperatures display nonuniform profiles along the direction normal to the wall, in particular, the temperature profiles are different for the two species while the temperature ratio is almost constant with the height. Finally, we obtained the velocity distributions at different heights and verified the non-Gaussianity of the resulting distributions.

DOI: 10.1103/PhysRevE.66.051304 PACS number(s): 81.05.Rm, 02.50.Ey, 05.20.Dd

I. INTRODUCTION

Granular materials present a rich and intriguing phenomenology, which has attracted the interest of the scientific community since the nineteenth century [1]. However, in spite of its recent progress the theoretical study of granular gases, i.e., of fluidized granular particles, is certainly less advanced than that concerning ordinary molecular fluids. The reason for this state of affairs is the presence of dissipation due to inelastic collisions and of friction with the surroundings, which prevents these system to reach thermodynamic equilibrium. In fact, in order to render stationary a granular system, one needs to inject energy continuously into the system. This can be done, for instance, by shaking or vibrating the grains.

In the present paper we illustrate the results of a numerical investigation concerning the properties of a two-component granular mixture, modeled, following an established tradition, by inelastic hard spheres (IHS) with different masses, restitution coefficients, radii, and subject to different forms of external drive. The physical motivation for our study stems from the fact that in nature most granular materials are polydisperse from the point of view of their sizes and/or of their physical and mechanical properties. The theoretical study of granular mixtures has attracted so far the attention of several researchers [2–5]. These studies comprehend both freely cooling and uniformly heated granular mixtures, and have been performed almost contemporaneously with laboratory experiments [6,7]. The most striking outcome is the lack of energy equipartition, i.e., the presence of two different kinetic temperatures, one for each species.

The salient features of the present work are the following:

(1) A finite-temperature uniform heat bath to drive the system was utilized. This is achieved by means of a finite friction between the particles and the surroundings.

(2) We also considered a situation in which the particles subject to a vertical gravitational field receive energy anisotropically from the bottom vibrating wall of the container.

(3) In both cases we provide information about the presence of inhomogeneities in the system, e.g., density clustering and nonuniform density and temperature profiles.

In Sec. II we present the model fluid and two different mechanisms of energy supply. In Sec. III we discuss the first submodel, the one with the heat bath, and obtain by means of an approximate analytic method an estimate of the partial temperature of each component. Subsequently we study the same submodel with a direct simulation Monte Carlo (DSMC) algorithm. In Sec. IV we study numerically the second submodel (the one with gravity and vibrating wall) by means of the DSMC [8,9]. Finally, in Secs. V and VI, we discuss the results and present our conclusions.

II. DEFINITION OF THE MODELS

We shall consider a dilute inelastic gas constituted of N_1 particles of mass m_1 and N_2 particles of mass m_2 subject to some kind of external driving (this will be specified in the following). We suppose that the interactions between the grains can be described by the smooth IHS model [10], thus we specify only the radius of the spheres, their masses and the fraction of the kinetic energy dissipated at each collision. This can be done by defining three different restitution coefficients α_{ij}, i.e., α_{11}, α_{22}, and $\alpha_{12}=\alpha_{21}$, which account for normal dissipation in collisions among particles of types i and j. No internal degrees of freedom (e.g., rotations) are included.

One can describe the velocity changes induced by the instantaneous inelastic collisions of smooth disks labeled 1 and 2 of diameters σ_1 and σ_2 by the following equations:

$$\mathbf{v}_1' = \mathbf{v}_1 - \frac{1+\alpha_{\kappa_1\kappa_2}}{2}\frac{m_{\kappa_2}}{m_{\kappa_1}+m_{\kappa_2}}[(\mathbf{v}_1-\mathbf{v}_2)\cdot\hat{\mathbf{n}}]\hat{\mathbf{n}}, \qquad (1a)$$

 ©2002 The American Physical Society

$$\mathbf{v}_2' = \mathbf{v}_2 + \frac{1+\alpha_{\kappa_1\kappa_2}}{2}\frac{m_{\kappa_1}}{m_{\kappa_1}+m_{\kappa_2}}[(\mathbf{v}_1-\mathbf{v}_2)\cdot\hat{\mathbf{n}}]\hat{\mathbf{n}}, \quad (1b)$$

where $\hat{\mathbf{n}}=2(\mathbf{x}_1-\mathbf{x}_2)/(\sigma_{\kappa_1}+\sigma_{\kappa_2})$ is the unit vector along the line of centers $\mathbf{x}_1$ and $\mathbf{x}_2$ of the colliding disks at contact and κ_1,κ_2 are the species (1 or 2) to which particles 1 and 2 belong. An elementary collision conserves the total momentum and reduces the relative kinetic energy by an amount proportional to $(1-\alpha^2_{\kappa_1\kappa_2})/4$. The collision rule we have adopted excludes the presence of tangential forces, and hence the rotational degrees of freedom do not contribute to the description of the dynamics.

Since the particles suffer mutual collisions and loose kinetic energy, in order to achieve a steady state, one needs to supply some energy from the exterior. The energy source has been modeled in two different fashions. In the first submodel we have assumed that the particles experience a uniform stochastic force and a viscous damping [11,12]. The presence of the velocity-dependent term, in addition to the random forcing, not only is motivated by the idea of preventing the energy of a driven elastic system ($\alpha_{\kappa_1\kappa_2}\to 1$), to increase indefinitely, but also mimics the presence of friction of the particles with the container. A fluctuation dissipation relation is assumed between the viscous force and the intensity of the noise. Even in extended systems with small inelasticity, the absence of friction may cause some problems of stability [15].

In the second submodel the grains are constrained to move on a frictionless inclined plane and the bottom boundary vibrates (as a thermal [13] or deterministic [14] oscillating wall). Periodic boundary conditions are assumed laterally.

Since we consider throughout only sufficiently low density systems, successive binary collisions are effectively uncorrelated and Boltzmann equation can be used to describe the nonequilibrium dynamics.

III. UNIFORMLY HEATED SYSTEM

In order to see the effect of the heat bath, let us consider the system in the absence of collisions. In this case, the evolution of the velocity of each particle is described by an Ornstein-Uhlenbeck process. If we require that the two components must reach the same granular temperature in the limit of vanishing inelasticity, we have two different possibilities to fix the heat-bath parameters:

$$\partial_t \mathbf{x}_i(t) = \mathbf{v}_i(t), \quad (2)$$

$$m_i\partial_t \mathbf{v}_i(t) = -\gamma\mathbf{v}_i(t) + \sqrt{2\gamma T_b}\xi_i(t), \quad (3a)$$

$$m_i\partial_t \mathbf{v}_i(t) = -m_i\eta\mathbf{v}_i(t) + \sqrt{2m_i\eta T_b}\xi_i(t), \quad (3b)$$

where $i=1,2$; T_b is the heat bath temperature; and $\xi(t)$ is a Gaussian noise with the following properties:

$$\langle \xi_i(t)\rangle = 0, \quad (4a)$$

$$\langle \xi_i(t_1)\xi_j(t_2)\rangle = \delta(t_1-t_2)\,\delta_{ij}. \quad (4b)$$

The associated Fokker-Planck equations for the two cases are, respectively,

$$\partial_t f_i(\mathbf{r},\mathbf{v},t) = \frac{\gamma}{m_i}\nabla_v(\mathbf{v}f_i(\mathbf{r},\mathbf{v},t)) + \frac{\gamma T_b}{m_i^2}\nabla_v^2 f_i(\mathbf{r},\mathbf{v},t) + \mathbf{v}\nabla_r f_i(\mathbf{r},\mathbf{v},t), \quad (5a)$$

$$\partial_t f_i(\mathbf{r},\mathbf{v},t) = \eta\nabla_v(\mathbf{v}f_i(\mathbf{r},\mathbf{v},t)) + \frac{\eta T_b}{m_i}\nabla_v^2 f_i(\mathbf{r},\mathbf{v},t) + \mathbf{v}\nabla_r f_i(\mathbf{r},\mathbf{v},t). \quad (5b)$$

A. Spatially uniform solutions

When we take into account collisions among particles, Eqs. (5) become two coupled Boltzmann equations modified by the presence of a diffusion term due to the thermal noise. In order to derive the temperature of each species in the homogeneous stationary state, we shall first neglect the spatial dependence of the distribution functions f_i. This can be regarded as a mean field approximation to the Boltzmann equation. In other words, we let collisions to occur regardless their spatial separation. Although the method of derivation of the equations for the partial temperatures is not original, we present it in order to render the paper self-contained and because it shows the differences between the particular heat bath we employed and those chosen by other authors [4]. First, indicating by $n_i=N_i/V$ the partial density of species i, we notice that both Eqs. (5) possess the same equilibrium solution:

$$f_i(\mathbf{v}) = n_i\left(\frac{m_i}{2\pi T_b}\right)^{d/2} e^{-m_i v^2/2T_b}, \quad (6)$$

but their relaxation properties are different. Only upon adding the inelastic collision term, the two species display different temperatures. The resulting Boltzmann equation for a granular mixture [2–4] is

$$\partial_t f_i(\mathbf{v}_1;t) = \sum_j J_{ij}[\mathbf{v}_1|f_i,f_j] + \frac{\xi_{0i}^2}{2}\nabla_v^2 f_i + \eta_i\nabla_v\cdot(\mathbf{v}_1 f_i), \quad (7)$$

where we have used a compact notation to represent the two different choices of heat bath:

In case 1,

$$\xi_{0i}^2 \to \frac{2\gamma T_b}{m_i^2}, \qquad \eta_i \to \frac{\gamma}{m_i}; \quad (8)$$

in case 2,

$$\xi_{0i}^2 \to \frac{2\eta T_b}{m_i},$$

$$\eta_i \to \eta; \tag{9}$$

and $J_{ij}[v_1|f_i,f_j]$ is the collision integral,

$$J_{ij}[v_1|f_i,f_j] \equiv \sigma_{ij}^2 \int d\mathbf{v}_2 \int d\hat{\boldsymbol{\sigma}}\Theta(\hat{\sigma}\cdot\mathbf{g}_{12})(\hat{\sigma}\cdot\mathbf{g}_{12}) \times[\alpha_{ij}^{-2} f_i(\mathbf{v}_1')f_j(\mathbf{v}_2') - f_i(\mathbf{v}_1)f_j(\mathbf{v}_2)]. \tag{10}$$

The primed velocities are precollisional states, which can be obtained by inverting Eqs. (1).

Due to the presence of the heat-bath terms, the system reaches asymptotically a steady state, characterized by time-independent pair distribution functions (pdf's). By requiring stationarity and integrating over $\mathbf{v}_1$ the equation for $v_i^2 f_i$, we obtain

$$\sum_j \int d\mathbf{v}_1 v_1^2 J_{ij}[\mathbf{v}_1|f_i,f_j] + \frac{\xi_{0i}^2}{2}\int d\mathbf{v}_1 v_1^2 \nabla_v^2 f_i + \eta_i \int d\mathbf{v}_1 v_1^2 \boldsymbol{\nabla}_v\cdot(\mathbf{v}_1 f_i) = 0. \tag{11}$$

After simplifying the second and the third integral by integration by parts and using the normalization property $\int f_i dv_i = n_i$, we find

$$\sum_j \int d\mathbf{v}_1 v_1^2 J_{ij}[\mathbf{v}_1|f_i,f_j] + n_i d\xi_{0i}^2 - 2\eta_i \int d\mathbf{v}_1 v_1^2 f_i(\mathbf{v}_1) = 0. \tag{12}$$

The partial temperature is defined as

$$n_i T_i \equiv \frac{1}{d}\int d\mathbf{v}_1 m_i v_1^2 f_i, \tag{13}$$

so that Eq. (12) can be recast as

$$T_i = \frac{m_i}{2d\eta_i}\left(\frac{1}{n_i}\sum_j \int d\mathbf{v}_1 v_1^2 J_{ij}[v_1|f_i,f_j] + d\xi_{0i}^2\right). \tag{14}$$

Equation (14) determines the partial temperatures once the f_i are known. In practice, one can obtain an estimate of T_i by substituting two Maxwell distributions:

$$f_i(v) = n_i\left(\frac{m_i}{2\pi T_i}\right)^{d/2} e^{-m_i v_1^2/2T_i}.$$

After performing the remaining integrals (see Refs. [2,4]), one gets

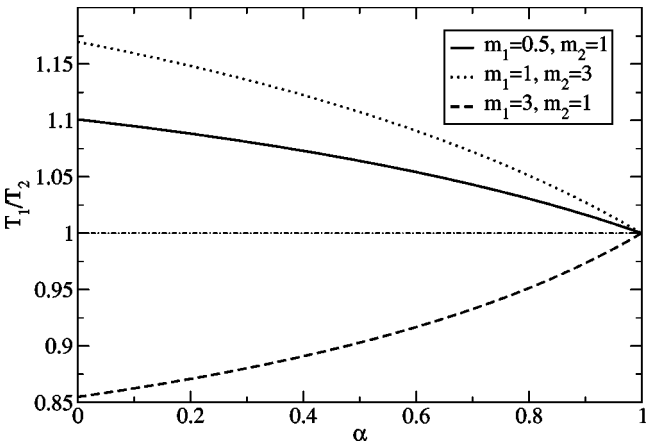

FIG. 1. Homogeneous driving. Granular temperature ratio T_1/T_2 vs α, obtained with the heat bath of case 1 using $T_b=1$, $\gamma=0.1$, and different mass ratios.

$$\frac{d\Gamma(d/2)}{m_i\pi^{(d-1)/2}} 2\eta_i(T_b - T_i) = \sigma_{ii}^{d-1} n_i \frac{2(1-\alpha_{ii}^2)}{m_i^{3/2}} T_i^{3/2} + \sigma_{ij}^{d-1} n_j \mu_{ji}\left[\mu_{ji}(1-\alpha_{ij}^2)\left(\frac{2T_i}{m_i}+\frac{2T_j}{m_j}\right) + 4(1+\alpha_{ij})\frac{T_i - T_j}{m_1+m_2}\right]\left(\frac{2T_i}{m_i}+\frac{2T_j}{m_j}\right)^{1/2}, \tag{15}$$

where $\mu_{ij} = m_i/(m_i+m_j)$. One obtains the steady values of the partial temperatures in the spatially homogeneous situation, by solving numerically the nonlinear system of Eqs. (15).

B. Comparison between the two heat baths

In Figs. 1 and 2, we report on the temperature ratio T_1/T_2 as a function of a common restitution coefficient α, having

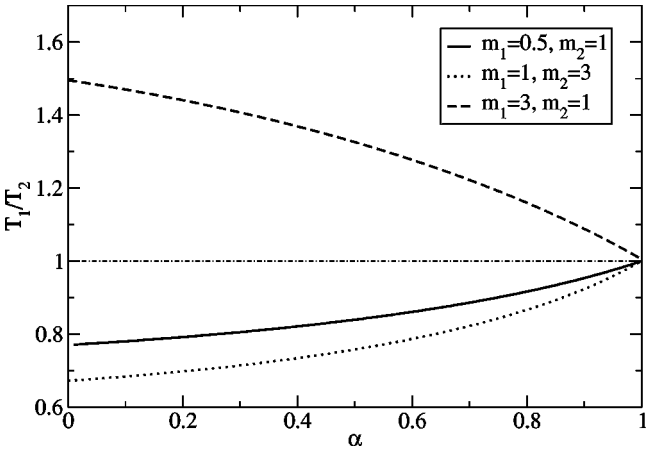

FIG. 2. Homogeneous driving of case 2. Granular temperature ratio T_1/T_2 vs α, with $T_b=1$, $\eta=0.1$, and various mass ratios.

chosen equal coefficients $\alpha_{11}=\alpha_{22}=\alpha_{12}=\alpha$. Assuming identical concentrations and varying the mass ratio m_1/m_2, we considered cases 1 and 2.

In the first case, the species with the largest mass is ''colder.'' In fact, both components receive the same energy from the heat bath, but the heavier species dissipates more energy due to collisions.

We notice that, on the contrary in case 2, the temperature ratio is, on the contrary, an increasing function of the mass ratio m_1/m_2. The experimental observation [6] suggest that the trend of case 2 is physically more relevant. In case 2, both the friction term and the power supplied are proportional to the mass of the two species. In the following DSMC simulations we shall use case 2.

C. DSMC of homogeneously driven systems

In the present section we illustrate the results obtained simulating the system with the heat bath [with recipe 2, i.e., Eq. (3b)] by the so-called direct simulation Monte Carlo, according to the implementation described in Ref. [16]. In this way we do not constrain the system to be spatially homogeneous since DSMC allows for fluctuations of the relevant fields.

At every time step of length Δt, each particle is selected to collide with a probability $p_c=\Delta t/\tau_c$ (where τ_c is an *a priori* fixed mean free time established consistently with the mean free path and mean squared velocity) and seeks its collision partner among the other particles in a neighborhood of radius r_B, choosing it randomly with a probability proportional to their relative velocity. Moreover, in this approximation the diameter σ is no more explicitly relevant, but it is directly related to the choices of p_c and r_B in a nontrivial way. In fact, the Bird algorithm allows the particles to pass through each other, so that a rigorous diameter cannot be defined or simply estimated as a function of p_c and r_B. In this section, to indicate the degree of damping, we give the time $\tau_b=1/\eta$ instead of η. This is useful to appreciate the ratio between the mean collision time τ_c and the mean relaxation time due to the bath, which indeed is τ_b.

In the present section we chose $N_1=N_2=500$ and $T_b=1$, and equal restitution coefficients for all collisions and $\tau_c=0.16$. As illustrated in Figs. 3 and 4, the two components display different granular temperatures in agreement with the analytical predictions of the homogeneous Boltzmann equations. We checked in our simulations that the ratio T_1/T_2 depends more on the mass ratio and much less on the asymmetries in the restitution coefficients, i.e., α_{11}/α_{22}. However, we do not observe the insensitivity of such a ratio with respect to inelasticity (e.g., changing $\alpha=\alpha_{11}\alpha_{22}$ as reported experimentally [6]). We shall comment such an issue below.

At a finer level of description we consider the rescaled velocity pdf for different values of the inelasticity parameter and different mass ratios $m_2/m_1=2$. One sees that not only the deviations from the Gaussian shape become more and more pronounced as we increase the inelasticity parameter $(1-\alpha)$, but also the shape of the two distributions differ appreciably in the tails even after velocity rescaling to make the two pdf's to have the same variance. One can also observe that the rescaled pdf of the lighter species has slightly broader tails. The mass ratio also controls the deviations from the Gaussianity of the velocity pdf's. It is well known that the departure from the Maxwell-Boltzmann statistics is triggered by the inelasticity of the collisions. The larger the inelasticity, the stronger is the deviation. The novelty in the case of mixtures is that the difference in the tails of the two velocity distributions increases as the inelasticity increases. Moreover, comparing Figs. 5 and 6 one sees that the mass asymmetry enhances the non-Gaussianity of the pdf. Such phenomena were predicted within a Maxwell model in Ref. [3].

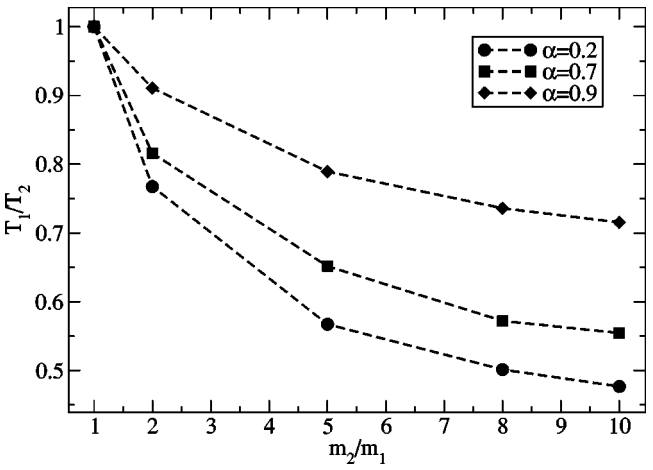

FIG. 3. Granular temperature ratios T_1/T_2 vs mass ratio m_2/m_1 for a binary mixture (DSMC simulation) with different values of α, $N_1=N_2=500$, $L^2=1000$, $T_b=1$, $\tau_b=10$, $\tau_c=0.16$, and case 2

We have also studied the limits of low and high τ_b, in Fig. 7, to show how the velocity distributions change. For values of the characteristic time of the heat bath, τ_b, comparable with the collision time τ_c, the dynamics is essentially controlled by the stochastic acceleration term. This fact renders the two partial temperatures very close and makes

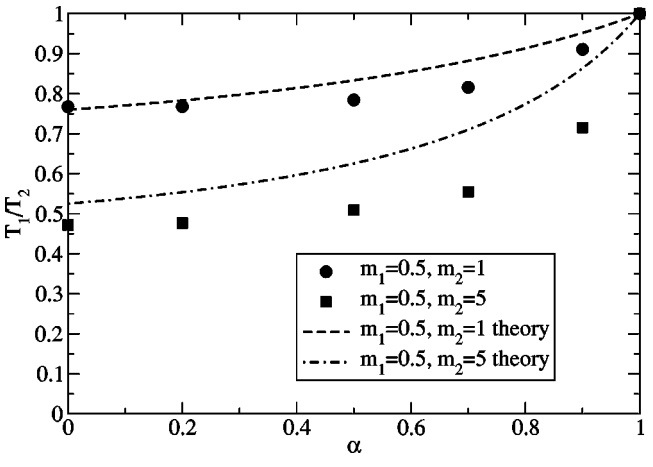

FIG. 4. Granular temperature ratios T_1/T_2 vs restitution coefficient α for a binary mixture (DSMC simulation) with different values of m_1/m_2, $N_1=N_2=500$, $L^2=1000$, $T_b=1$, $\tau_b=10$, $\tau_c=0.16$, and case 2. The dashed lines represent the temperature ratios predicted by Eq. (15) with case 2.

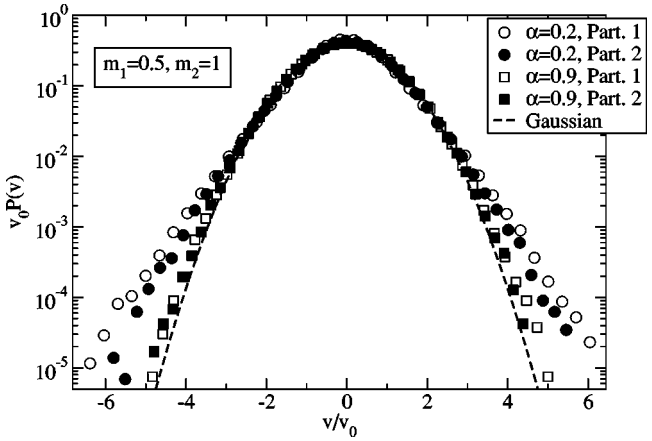

FIG. 5. Rescaled (to have variance 1) velocity distributions $P(v)$ vs v in the numerical experiment with the thermal bath (DSMC simulation), for binary mixtures of particles with masses $m_1=0.5$ and $m_2=1$, with $N_1=N_2=500$, $L^2=1000$, $T_b=1$, $\tau_b=10$, $\tau_c=0.16$, case 2, and different values of α.

the velocity distributions nearly Maxwellian. As τ_b increases, we have observed that the energy dissipation due to the inelasticity makes the temperatures of the two species different. Moreover, the temperature ratio displays the power law decreasing trend as a function of τ_b, whose strength depends on the mass ratio (see Fig. 8).

In order to obtain information about the spatial structure of the mixture, we have performed an analysis of the following correlation function that is already introduced in the context of granular media by [11,12,17] (see Fig. 9)

$$C_{\alpha\eta}(r)=\frac{1}{N(N-1)}\sum_{i\neq j}\Theta(r-|\mathbf{x}_i^{\alpha}-\mathbf{x}_j^{\eta}|). \qquad (16)$$

For a spatially homogeneous system we expect that $C_{\alpha\eta}(r)\approx r^{d_2}$, with $d_2=d$ being the dimension of the embedding space. When $\tau_b<\tau_c$, we observe that $d_2=2$, as expected for a homogeneous (i.e., uncorrelated) density. This is due to the fact that the homogeneous driving dominates the dynamics, and the collisions have small effect on it; it is also consistent with the restoration of Maxwellian distribution of velocities (see Fig. 7). When $\tau_b>\tau_c$ we observe that $d_2<2$, which is a signature of fractal density clusterization. Moreover, one can also appreciate a small difference in the $C(r)$ relative to the two species, indicating a different level of clusterization, the heavier species is more clusterized than the lighter one.

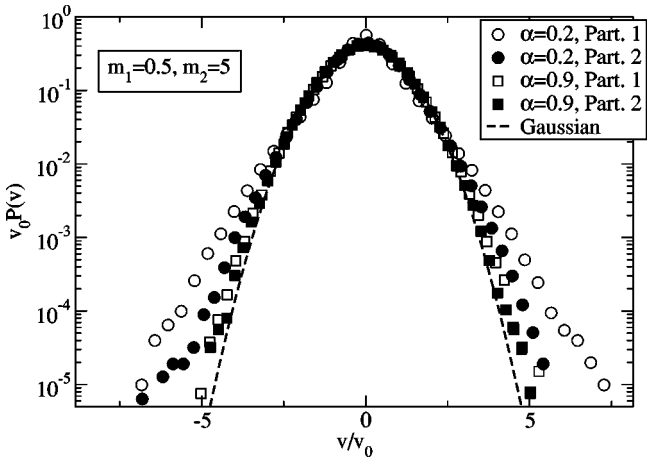

FIG. 6. Rescaled (to have variance 1) velocity distributions $P(v)$ vs v in the numerical experiment (DSMC simulation) with the thermal bath, for binary mixtures of particles with masses $m_1=0.5$ and $m_2=5$, with $N_1=N_2=500$, $L^2=1000$, $T_b=1$, $\tau_b=10$, $\tau_c=0.16$, case 2, and different values of α.

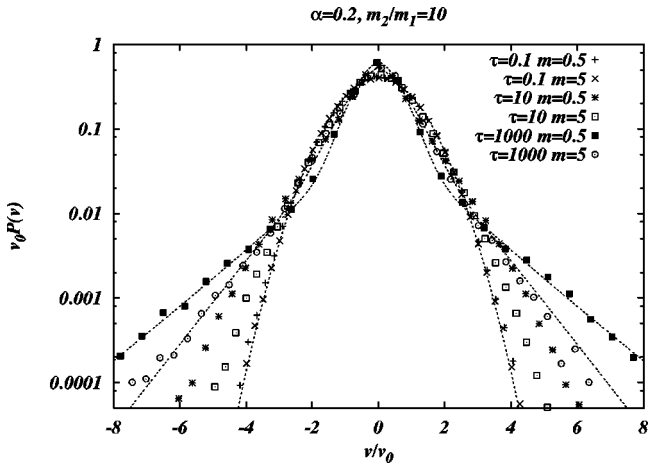

FIG. 7. Rescaled (to have variance 1) velocity distributions $P(v)$ vs v in the numerical experiment (DSMC simulation) with the thermal bath, for binary mixtures of particles with masses $m_1=0.5$ and $m_2=5$, with $N_1=N_2=500$, $L^2=1000$, $\alpha=0.2$, $T_b=1$, different values for τ_b, $\tau_c=0.16$, and with case 2.

IV. SYSTEM WITH GRAVITY

A. Setup

We turn, now, to illustrate the results relative to an inelastic mixture subject to gravity, and confined to a vertical plane

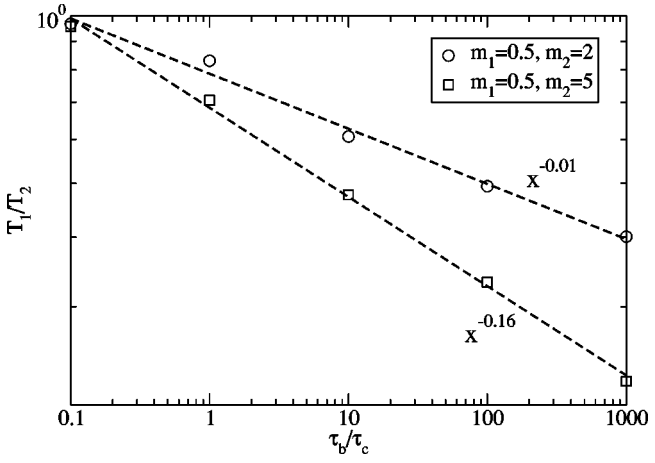

FIG. 8. Temperature ratios T_1/T_2 vs the rescaled viscosity time τ_b/τ_c (with fixed $\tau_c=0.16$) in the numerical experiment (DSMC simulation), with the thermal bath for a binary mixture of particles with masses $m_1=0.5$ and $m_2=5$, with $N_1=N_2=500$, $L^2=1000$, $\alpha=0.2$, $T_b=1$, different mass ratios, with case 2, and different values of α.

of dimensions $L_x \times L_y$. In the horizontal direction x, we assumed periodic boundary conditions. Vertically, the particles are confined by walls. Energy is supplied by the bottom wall vibrating stochastically or periodically according to the method employed in Ref. [16] for a one component system.

The vibration can have either a periodic character (as in Ref. [18]) or a stochastic behavior with thermal properties (as in Ref. [13]). In the periodic case, the wall oscillates vertically with the law $Y_w = A_w \sin(\omega_w t)$, and the particles collide with it as with a body of infinite mass with restitution coefficient α_w, so that the vertical component of their velocity after the collision is $v_y' = -\alpha_w v_y + (1+\alpha_w) V_w$, where $V_w = A_w \omega_w \cos(\omega_w t)$ is the velocity of the vibrating wall. In the stochastic case we assume that the vibration amplitude is negligible, and that the particles colliding with the wall have, after the collision, new random velocity components $v_x \in (-\infty, +\infty)$ and $v_y \in (0, +\infty)$, with the following probability distributions:

$$P(v_y) = \frac{v_y}{T_w} \exp\left(-\frac{v_y^2}{2T_w} \right), \tag{17}$$

$$P(v_x) = \frac{1}{\sqrt{2\pi T_w}} \exp\left(-\frac{v_x^2}{2T_w} \right). \tag{18}$$

In this model we assume that the particles do not feel any external (environmental) friction. In all the simulations, we have chosen $N_1 = N_2 = 100$, $g = 1$, $m_1 = m_2/2 = 1/4$, and $L_x = L_y = L = \sqrt{N}$.

The Boltzmann equations for the partial distribution functions $f_\kappa(\mathbf{r}, \mathbf{v}; t)$ with $\kappa = 1,2$ read

$$\left(\frac{\partial}{\partial t} + \mathbf{v} \cdot \boldsymbol{\nabla}_r + g_i \frac{\partial}{\partial v_i} \right) f_\kappa(\mathbf{r}, \mathbf{v}, t) = \sum_\eta J_{\kappa\eta}(f_\kappa, f_\eta). \tag{19}$$

B. Profiles

The results of DSMC simulations show that the tendency of the grains to form clusters is enhanced by such a choice of driving mechanism with respect to the homogeneous heat bath of the preceding section. In the latter, the noise acting uniformly was more effective in breaking the clusters. In addition, the gravitational force tends to group the particles in the lower portion of the container for driving frequencies not too large [16].

Figure 10 illustrates the partial density profiles and granular temperature profiles in the presence of a thermal wall of intensity $T_p = 20$. The density profiles differ slightly near the bottom wall where both present a maximum (see inset). The temperature profiles are different, putting again in evidence a strong lack of equipartition in the system. Interestingly, the temperature ratio is almost constant along the vertical direction, notwithstanding the partial profiles are nonconstant. We have also performed numerical simulations with a harmonically vibrating wall, as the maximum velocity of the vibrating wall (which, for $A = 1$, is equal to ω) increases, the position of the density maximum raises, indicating that gravity becomes less and less relevant. As far as the partial temperatures are concerned, Fig. 11 illustrates the corresponding situation.

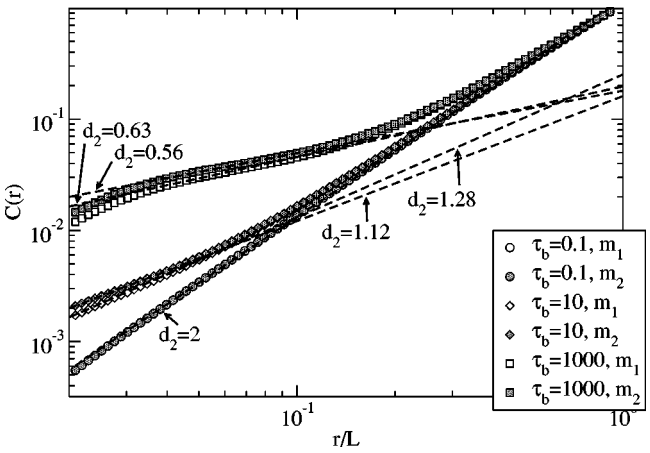

FIG. 9. Correlation function used to compute the correlation dimension d_2, $C(r)$ vs r (see text for definition), for a binary mixture (DSMC simulation) with $m_1 = 0.5$, $m_2 = 5$, $\tau_c = 0.16$, $T_b = 1$, $N_1 = N_2 = 500$, $L^2 = 1000$, $\alpha = 0.2$, and with different values for τ_b.

One sees that first the temperatures (see inset) next to the wall attain their largest value, but then drop to increase again. This indicates that the region far from the bottom is hotter because of the lower density of the gas and of the lower collision rate. As the wall temperature increases, the temperature becomes more homogeneous far from the bottom due to the major homogeneity in density. We also notice a small segregation effect.

The value obtained by our simulation for the temperature ratio (having chosen $m_1/m_2 = 0.3$ and a single restitution coefficient $\alpha = 0.93$), is $T_1/T_2 \approx 0.75$, and is not too far from the value obtained experimentally by Feitosa and Menon [6], which is 0.66 ± 0.06. One should recall that in our ''setup''

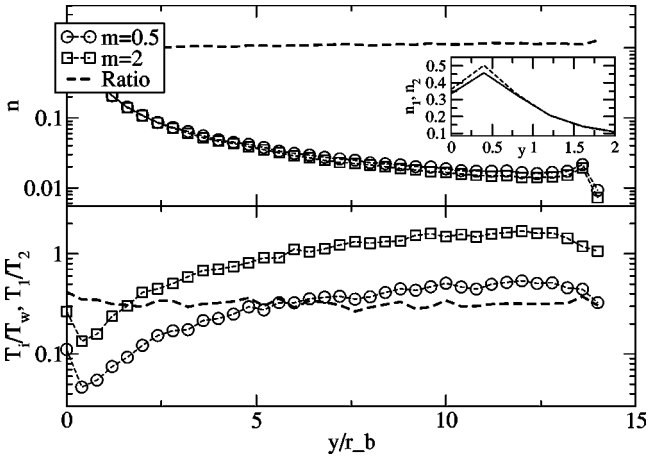

FIG. 10. Profiles for probability density per unit length $n(y)$ [i.e., $\int n(y)dy = 1$] and rescaled granular temperature $T(y)/T_w$ vs the rescaled vertical position y/r_b for a binary mixture with $m_1 = 0.5$, $m_2 = 2$, on an inclined plane with a thermal bottom wall (DSMC simulation) with $T_w = 20$, $N_1 = N_2 = 100$, $L^2 = 200$, $\alpha = 0.6$, $\alpha_w = 1$, $g = 1$; the dashed lines indicate the ratios for both profiles.

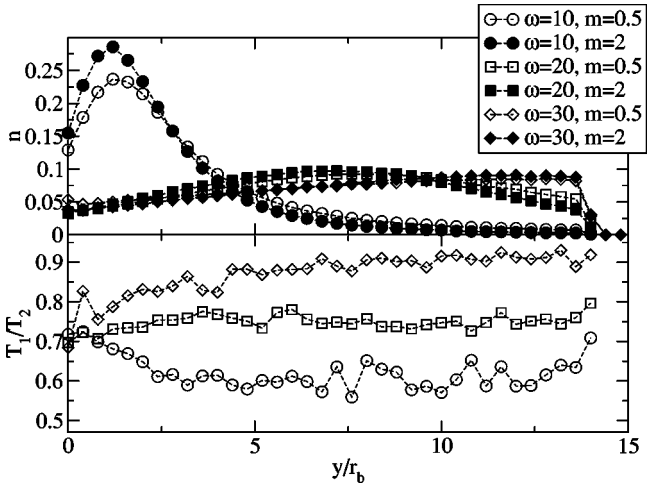

FIG. 11. Profiles for probability density per unit length $n(y)$ [i.e., $\int n(y)dy=1$] vs the rescaled vertical position y/r_b and ratios between granular temperatures of the two species $T_1(y)/T_2(y)$ vs y/r_b, for a binary mixture (DSMC simulation) with $m_1=0.5$ and $m_2=2$, on an inclined plane with a harmonically oscillating bottom wall with $A=1$, different values of ω, $N_1=N_2=100$, $L^2=200$, $\alpha=0.9$, and $\alpha_w=\alpha g=1$.

only the lower wall supplies energy to the system, whereas in the experiment both walls vibrate.

C. Velocity distributions

Finally, we present the velocity distributions measured in the system with a thermal wall. Since the temperature depends on the vertical coordinate y we have computed the velocity pdf's at different heights. The various pdf's are plotted in Fig. 12 after a suitable rescaling. We observe that the distributions deviate appreciably from a Gaussian shape and display overpopulated high-energy tails.

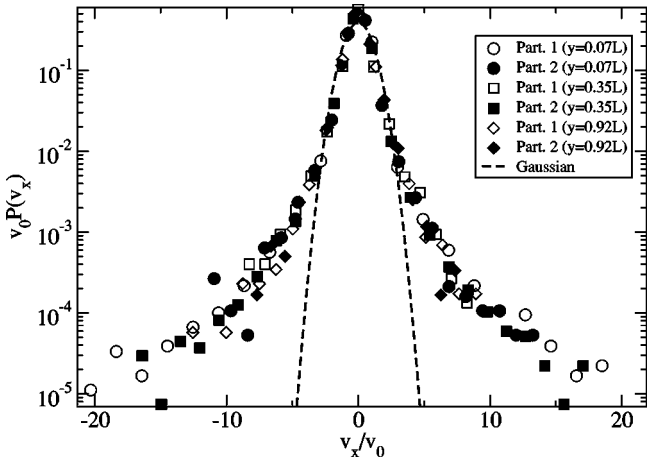

FIG. 12. Rescaled distributions (to have variance 1) of velocity $P(v)$ vs v for particles taken in stripes at different heights, for a binary mixture (DSMC simulation) with $m_1=0.5$, $m_2=2$, on an inclined plane with a thermal bottom wall with $T_w=20$, $N_1=N_2=100$, $L^2=200$, $\alpha=0.6$, and $g=1$.

V. DISCUSSION

The present numerical results not only confirm the predictions of different temperatures for the two species for all types of drive, but also show the existence of different shape functions for the velocity distributions of the two species and of overpopulated high-energy tails in agreement with the findings based on Maxwell models [3].

In order to obtain a comparison with experiments, we employed parameters comparable to those utilized in the experimental work of Ref. [6] and found only qualitative agreement. First, one should expect that due to the assumptions underlying the Boltzmann equation, the density profiles computed numerically are not accurate, and that a better treatment of the excluded volume effect is necessary in order to obtain a more realistic description of the system. In particular, the dense region is not accurately described. These density profiles in turn affect the shape of the temperature profiles. Finally, in view of the approximations inherent to the Boltzmann approach, we have neither tried to include the effect of rotations of the grains nor the friction with the lateral walls, which might be both relevant [19].

As far as the physical origin of the lack of kinetic energy, equipartition formula (15) seems to contain the right dependence on the various parameters in the homogeneous case, but its interpretation is not immediate. Plotting Eq. (15) numerically, one sees that the dependence of T_1/T_2 upon the composition is rather weak, as shown experimentally and noted by Barrat and Trizac [20]. Heuristically, we argue that the difference between T_1 and T_2 is determined primarily by the energy source (the vibrating wall) that transmits energies proportional to the mass of each species. Second, the dissipative forces may or may not tend to restore the energy equipartition. For instance, if the heavier species is more inelastic, the ratio may be close to unity; and this is due to the presence of two competing effects. On the contrary, if the heavier species is more elastic, the ratio will deviate appreciably from unity. Due to the simplicity of the present treatment, we did not explore the range of inelasticity parameters necessary to obtain a better fit to the experiments. We reached the conclusion that, in spite of the general qualitative agreement between our model and the experiments, we have no evidence to support completely the conjecture of Feitosa and Menon about the insensitivity of the temperature ratio on the inelasticities. Possible explanations are the following:

(1) There are other ingredients missing in the theoretical model employed, such as internal deformations of the spheres, etc.

(2) The effective inelasticity of the glass spheres might become less than the one assumed (the suggested restitution coefficient of glass is 0.9).

(3) We have employed a single vibrating wall instead of two walls.

VI. CONCLUSIONS

To summarize, we have studied the steady state properties of a granular mixture subject to two different classes of external drive.

In the case of a heat bath acting homogeneously on the

grains, we have first obtained the temperatures of each species by employing an approximate analytic method. We have then solved numerically the equations by allowing the density and the temperatures to be spatially varying, and analyzed the spatial correlations and the velocity distributions. The heavier species showed a higher degree of clusterization since it dissipates more energy. Finally, we turned to investigate the properties of the mixture in the presence of gravity and of a vibrating base. The properties of such system were not very sensitive to the choice of the law according to which the wall moves. For this setup we have obtained partial density profiles and partial temperature profiles, and noticed only a small segregation with the lighter particles at the top.

The rescaled velocity distribution functions in the presence of gravity appear to be broader than the corresponding quantities in the presence of homogeneous heating. The stronger the collisional energy loss with respect to the energy injection, the more evident the phenomenon.

As a general rule for the temperatures, we observed strong deviation from the equipartition when the heavy particles are also the more elastic, while such a deviation can be small if the heavy particles are the more elastic.

ACKNOWLEGMENTS

This work was supported by Ministero dell'Istruzione, dell'Università e della Ricerca, Cofin 2001 Prot. 200102384. A.P. acknowledges support from the INFM Center for Statistical Mechanics and Complexity (SMC).

[1] For a general overview, see H. M. Jaeger, S. R. Nagel, and R. P. Behringer, Rev. Mod. Phys. **68**, 1259 (1996), and references therein.
[2] Vicente Garzó and James Dufty, Phys. Rev. E **60**, 5706 (1999).
[3] U. Marini Bettolo Marconi and A. Puglisi, Phys. Rev. E **65**, 051305 (2002); **66**, 011301 (2002).
[4] A. Barrat and E. Trizac, Granular Matter **4**, 57 (2002).
[5] S. R. Dahl, C. M. Hrenya, V. Garzó, and J. W. Dufty, e-print cond-mat/0205413.
[6] K. Feitosa and N. Menon, Phys. Rev. Lett. **88**, 198301 (2002).
[7] R. D. Wildman and D. J. Parker, Phys. Rev. Lett. **88**, 064301 (2002).
[8] G. A. Bird, *Molecular Gas Dynamics* (Clarendon, Oxford, 1976).
[9] G. A. Bird, *Molecular Gas Dynamics and the Direct Simulation of Gas Flows* (Clarendon, Oxford, 1994).
[10] C. S. Campbell and C. E. Brennen, J. Fluid Mech. **151**, 167 (1985).
[11] A. Puglisi, V. Loreto, U. Marini Bettolo Marconi, A. Petri, and A. Vulpiani, Phys. Rev. Lett. **81**, 3848 (1998).
[12] A. Puglisi, V. Loreto, U. Marini Bettolo Marconi, and A. Vulpiani, Phys. Rev. E **59**, 5582 (1999).
[13] M. Isobe and H. Nakanishi, Phys. Rev. E **64**, 031304 (2001); M. Isobe and H. Nakanishi, J. Phys. Soc. Jpn. **68**, 2882 (1999).
[14] A. Kudrolli and J. Henry, Phys. Rev. E **62**, R1489 (2000).
[15] U. Marini Bettolo Marconi and A. Puglisi (unpublished).
[16] A. Baldassarri, U. Marini Bettolo Marconi, A. Puglisi, and A. Vulpiani, Phys. Rev. E **64**, 011301 (2001).
[17] P. Grassberger and I. Procaccia, Phys. Rev. Lett. **50**, 346 (1983).
[18] A. Kudrolli and J. P. Gollub, in *Powder and Grains '97, Proceedings of the Third International Conference, Durham, SC, 1997*, edited by J. T. Jenkins and R. P. Behringer (Balkema, Rotterdam, 1997).
[19] D. Paolotti, C. Cattuto, U. Marini Bettolo Marconi, and A. Puglisi, e-print cond-mat/0207601.
[20] A. Barrat and E. Trizac, e-print cond-mat/0207267.